SURFACE AND INTERFACE ANALYSIS
Surf. Interface Anal. 2002; **33**: 570–576
Published online in Wiley InterScience (www.interscience.wiley.com). DOI: 10.1002/sia.1422

SIA

Soft x-ray absorption spectroscopy study of oxide layers on titanium alloys

M. F. López,[1]* L. Soriano,[2] F. J. Palomares,[1] M. Sánchez-Agudo,[2] G. G. Fuentes,[2] A. Gutiérrez[2] and J. A. Jiménez[3]

[1] Instituto de Ciencia de Materiales de Madrid, CSIC, Cantoblanco, E-28049 Madrid, Spain
[2] Departamento de Fisica Aplicada, Instituto de Materiales Nicolás Cabrera, Universidad Autónoma de Madrid, Cantoblanco, E-28049 Madrid, Spain
[3] Centro Nacional de Investigaciones Metalúrgicas, CSIC, Avda. Gregorio del Amo 8, E-28040 Madrid, Spain

Received 19 December 2001; Revised 23 March 2002; Accepted 2 April 2002

Soft x-ray absorption spectroscopy (XAS) has been used to perform chemical analysis of oxide films formed after contact with air, both at room temperature and at 750 °C, on three titanium alloys. The alloys investigated were Ti–13Nb–13Zr, Ti–15Zr–4Nb and Ti–7Nb–6Al. Soft x-ray absorption spectra were taken at the Ti 2p and O 1s edges. The spectra corresponding to the room-temperature-oxidized samples are similar for the three alloys and show the presence of native oxide with a small metallic contribution. For the heat-treated samples, the alloying elements as well as element diffusion play a significant role in the formation of the oxide layer. In this case, the spectra exhibit clear differences between the TiNbZr alloys and Ti–7Nb–6Al. The oxide layer of the two TiNbZr alloys for the different heat treatment times is composed of TiO_2 in the form of rutile. However, for Ti–7Nb–6Al short heat treatments give rise to the formation of Al_2TiO_5. By increasing the oxidation time, an Al_2O_3 layer grows on the initial oxide film, becoming thicker as the exposure time is enhanced. Copyright © 2002 John Wiley & Sons, Ltd.

KEYWORDS: x-ray absorption spectroscopy; Ti alloys; electronic structure; oxidation; corrosion

INTRODUCTION

Nowadays titanium and its alloys are materials widely used in technological applications owing to their excellent combination of mechanical properties and corrosion resistance.[1,2] The main advantage of these materials is the high strength/weight ratio, which is one of the highest among the metallic materials. On the other hand, the excellent corrosion resistance of pure Ti is the result of the spontaneous formation of a protective native oxide layer on its surface, called the passive layer.

Mechanical properties of Ti can be improved by alloying elements and by a microstructural modification through heat treatments.[3] The attractive combination of mechanical properties that can be developed make Ti alloys suitable for various technological applications in the aircraft and automotive industry or in biomaterial manufacturing.[4–6] The continuous need to improve the materials performance in these activities makes the development of new Ti alloys an active research field.[7]

*Correspondence to: M. F. López, Instituto de Ciencia de Materiales de Madrid, CSIC, Cantoblanco, E-28049 Madrid, Spain.
E-mail: mflopez@icmm.csic.es
Contract/grant sponsor: Programa de Tecnología de los Materiales de la Comunidad Autónoma de Madrid; Contract/grant number: 07N-0050-1999.
Contract/grant sponsor: MCYT, Spain; Contract/grant number: BFM 2000-0023.
Contract/grant sponsor: EU; Contract/grant number: HPRI-CT-1999-00028.

With regard to surface and corrosion properties, determination of the chemical composition of the passive layer formed on new Ti alloys is of high interest.[8,9] This layer is the result of the strong Ti affinity for oxygen and forms naturally when the alloy is exposed to air. This passive film provides, in most cases, an excellent resistance to corrosion. However, for some applications the protection against the environment can be improved by generating an oxide layer by heat treatment.

Soft x-ray absorption spectroscopy (XAS) can provide significant information on the chemical and electronic properties of matter.[10] Recently, this technique has also been devoted to some more technological materials.[11–16] In soft x-ray absorption an electron is excited from a core state to an empty state. The absorption cross-section is measured by detecting electrons or photons, which escape from the material after decay of the core hole. Because the core-level binding energies are well defined for each chemical element, this technique allows detailed element-specific studies. In the total electron yield (TEY) mode all escaping electrons are counted. The sampling depth of XAS in this mode is of the order of 70–100 Å for the transition metal 2p edges.[17,18] This range is larger than that of other more surface-sensitive techniques such as x-ray photoelectron spectroscopy (XPS). Although XPS in conjunction with ion sputtering is widely used to perform surface characterization,[19–21] in some cases this method must be applied carefully because the sputtering process can lead to reduction of the observed species. This is especially important in the case of passive and oxide

layers, where the presence of different metal oxides and chemical states is expected. In these cases, XAS is a more suitable technique because, owing to its sampling depth, no sputtering process can be carried out to study deeper surface layers. Thus, XAS in TEY mode permits adequate study of the chemical composition of the passive film of corrosion-resistant materials whose thickness is typically of the order of 30–60 Å.[12,14]

In the present article, we report on a soft XAS study of three Ti alloys: Ti–13Nb–13Zr, Ti–15Zr–4Nb and Ti–7Nb–6Al. The aim of this work is to perform a chemical analysis of the passive layer formed on these alloys spontaneously through air contact at room temperature as well as at high temperature. By applying XAS at the Ti 2p and the O 1s edges in TEY mode it is possible to obtain information on these oxides.

EXPERIMENTAL

Three titanium alloys with chemical composition (wt.%) Ti–13Nb–13Zr, Ti–15Zr–4Nb and Ti–7Nb–6Al were selected for the present study. Although the alloys will be named as determined by the weight per cent composition, the value of the atomic per cent composition is also important to interpret the results. Thus, for Ti–13Nb–13Zr, Ti–15Zr–4Nb and Ti–7Nb–6Al the compositions (at.%) are Ti–7.8Zr–7.7Nb, Ti–8.7Zr–1.3Nb and Ti–10.4Al–3.6Nb, respectively. The alloys were prepared by arc melting and subsequent casting in a copper coquille under high vacuum. The oxidation samples were cut from as-cast ingots by electrosparl-erosion. The surfaces of these samples were abraded and polished using diamond pastes with successively finer particle size. In order to ensure a surface free of mechanical deformation, this process was finished with colloidal silica. The material in this state was termed '*as received*'. At this stage, some samples were isothermally oxidized at 750 °C in air for three different exposure times: 90 min, 6 h and 24 h.

The XAS measurements were carried out at the VLS-PGM soft x-ray monochromator at the Berliner Elektronenspeicherring für Synchrotronstrahlung (BESSY). The monochromator resolution at the Ti 2p edge was better than 100 meV. The XAS spectra were obtained at the Ti 2p and the O 1s absorption thresholds by recording the total yield of electrons from the sample surfaces, i.e. in TEY mode. The base pressure in the ultra high vacuum (UHV) chamber during the measurements was better than 2×10^{-10} mbar.

RESULTS

Quantitative analysis by XAS

Figure 1 shows the survey spectra of the as-received and heat-treated Ti–7Nb–6Al alloy. In this figure different spectral features can be observed, which correspond to different absorption edges. Taking into account the binding energies of the core-level electrons, the determination of the absorption thresholds was easily done. Thus, the features located at ~458 eV and ~531 eV correspond to the Ti 2p and O 1s edges,

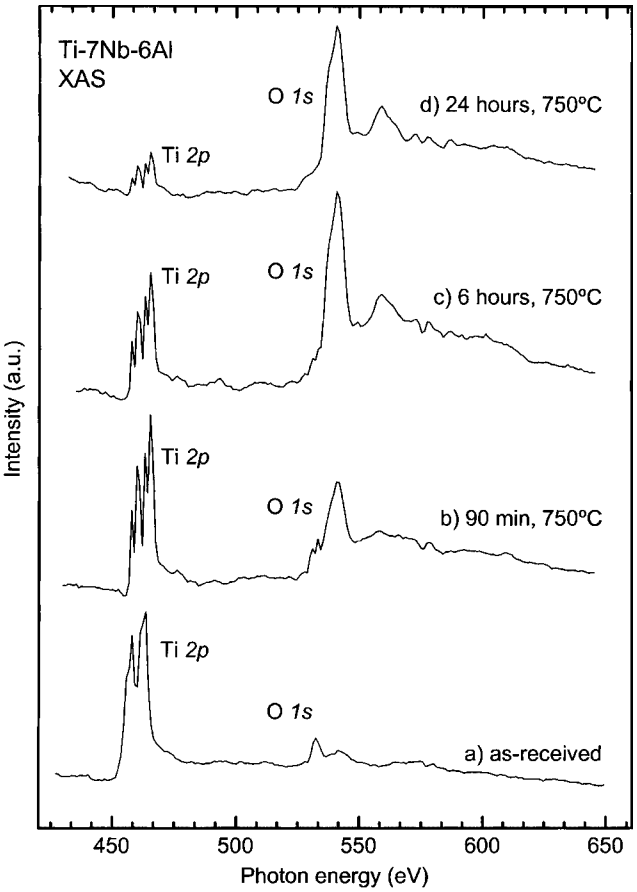

Figure 1. Broad XAS spectra of the as-received and heat-treated Ti–7Nb–6Al alloy.

Table 1. The Ti 2p/O 1s ratio for the near-surface region obtained for Ti–7Nb–6Al, Ti–13Nb–13Zr and Ti–15Zr–4Nb at different oxidation times

Oxidation time	Ti–7Nb–6Al	Ti–13Nb–13Zr	Ti–15Zr–4Nb
As-received	5.99	6.99	7.02
90 min	1.79	6.31	6.32
6 h	0.65	6.15	6.30
24 h	0.26	6.13	6.28

respectively. From these spectral data, a simple calculation can be made to estimate the Ti 2p/O 1s ratio for the near-surface region. The Ti/O values obtained for the as-received sample and heat-treated samples are presented in Table 1. For Ti–7Nb–6Al, the data show a strong Ti/O decrease when the heat treatment is applied, which continues with increase of exposure time. This behaviour, which is clearly observed in Fig. 1, suggests that other elements different to Ti are being continuously oxidized. For the TiNbZr alloys the survey spectra were also measured, and the calculated Ti 2p/Os 1s ratios exhibit similar behaviour that changes only slightly for the different spectra, in contrast with the Ti–7Nb–6Al case. In the two TiNbZr alloys, the Ti/O ratio obtained for all heat-treated samples is very similar, varying from 6.32 to 6.13 (see Table 1). However, the as-received sample exhibits a Ti/O value of ~7, which is slightly higher than that of the heat-treated samples. For both TiNbZr alloys,

these results suggest an initial change of the surface chemical composition when the oxidation treatment starts, with almost no variation on increasing the oxidation time.

The quantitative data extracted from the survey spectra suggest a different oxidation behaviour between the Ti–7Nb–6Al and TiNbZr alloys. In order to clarify the different phenomena that are taking place in these Ti alloys during thermal exposition at 750 °C, a more detailed study of the Ti 2p and O 1s absorption edges was performed.

The TiNbZr alloys

Figure 2 represents the Ti 2p XAS spectra of the as-received and heat-treated Ti–13Nb–13Zr alloy. The solid lines through the data points serve as a guide to the eye. The Ti 2p spectra correspond mainly to Ti 2p → 3d transitions. The spectra consist of two multiplets, one of them located at energies lower than ~461 eV and the other at energies higher than ~461 eV. These multiplets are separated, to a first approximation, by the spin-orbit splitting of the Ti 2p core hole. Owing to the crystal-field effects, the Ti 3d states split into two orbitals, t_{2g} and e_g. Consequently, this is reflected in the XAS spectra by an additional splitting of each multiplet into two features, resulting finally in four main peaks clearly observed in Fig. 2. As can be observed in this figure, the Ti 2p spectra of the three treated samples are similar whereas the as-received sample spectrum differs from them. The spectral shape of the heat-treated samples is typical of TiO_2, as can be deduced by comparison with previous works.[22,23] The shoulder of the e_g band, located at ~459.2 eV, indicates that TiO_2 is in the form of rutile. This shoulder is the result of the oxygen octahedron distortion in rutile, which causes an extra splitting in the e_g orbital. The as-received alloy spectrum is broader than the spectra of the three heat-treated samples and also shows a shift of the peak onset. Both characteristics are indications of the presence of metallic titanium.[24] Because the probe depth of XAS in TEY is larger than the thickness of the passive layer in these materials (30–60 Å), the metallic contribution from the substrate in the as-received Ti 2p spectrum is expected. The spectral shape is, however, very similar to that reported previously for the native oxide of FeTi alloys,[25] confirming the native oxide contribution. As mentioned above, Ti and its alloys develop a protective oxide layer on the surface that is responsible for their excellent corrosion resistance. Nevertheless, it is important to determine as precisely as possible the composition of this native oxide layer.

The O 1s XAS spectra of the as-received and heat-treated Ti–13Nb–13Zr alloy are displayed in Fig. 3. These spectra originate mainly from transitions into unoccupied states with O 2p character hybridized with metal states. Therefore, the spectral features can be related qualitatively to empty bands of primarily metallic character. Interpretation of the O 1s XAS spectrum must be done carefully because the possibility of oxide mixtures leads to peak overlap. However, as mentioned above, qualitative information can

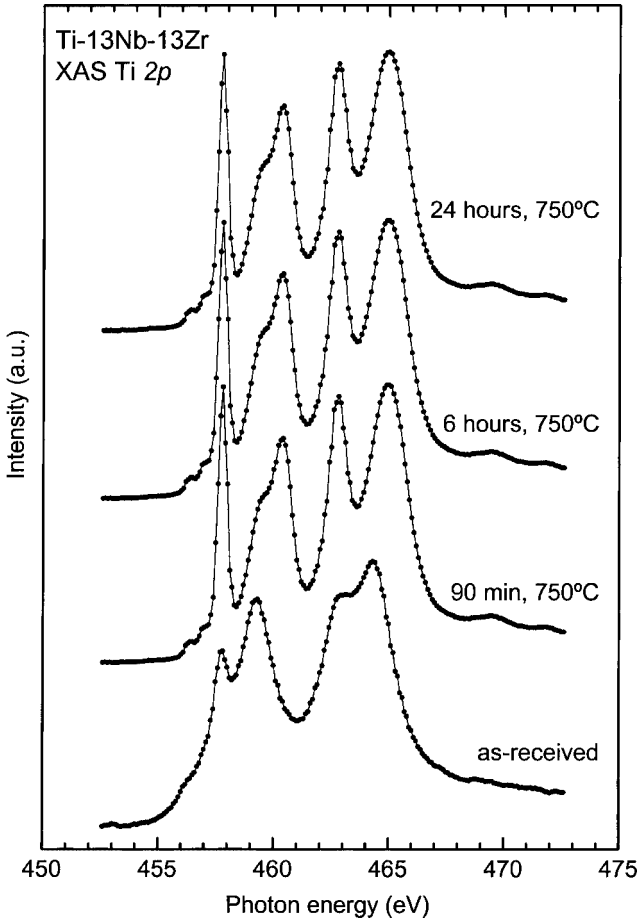

Figure 2. Titanium 2p soft x-ray absorption spectra of the as-received and heat-treated Ti–13Nb–13Zr alloy.

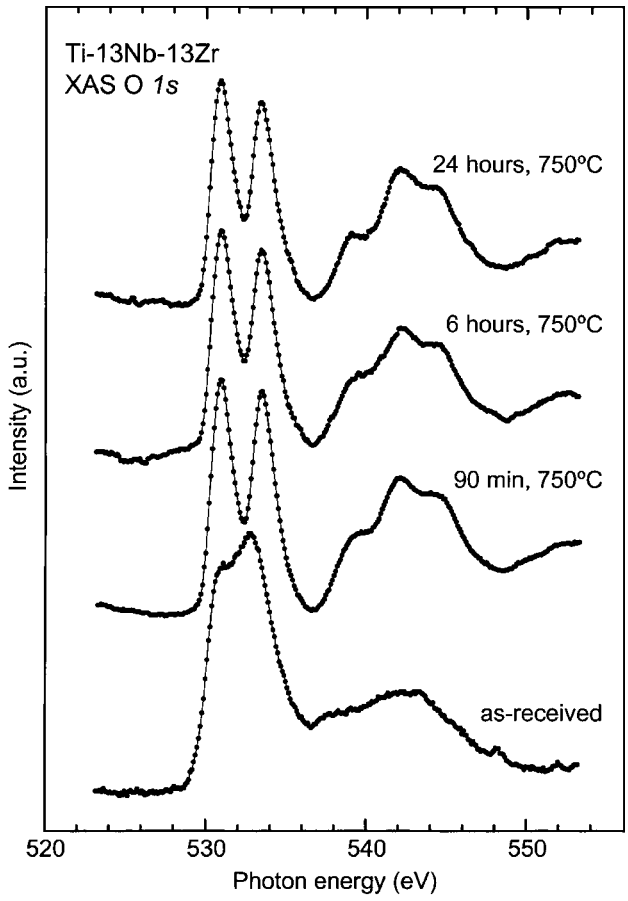

Figure 3. Oxygen 1s soft x-ray absorption spectra of the as-received and heat-treated Ti–13Nb–13Zr alloy.

be extracted from these data, which would complement the results obtained on the Ti 2p XAS spectra. The O 1s spectra can be divided into two regions. The first region at 525–536 eV is attributed to the O 2p weight in states of predominantly transition-metal d-character. This spectral region is quite sensitive to the local symmetry and to the ligand coordination. The second region at 536–548 eV is attributed to oxygen p-character hybridized with metal s- and p-states and is sensitive to long-range order. All heat-treated samples exhibit the typical O 1s spectrum of rutile (TiO_2),[24,26–29] which nicely agrees with the Ti 2p spectra discussed previously. Thus, the two peaks observed in the first region, with an energy separation of ~2.6 eV, are assigned to the t_{2g} and e_g orbitals of TiO_2, respectively. On the other hand, the as-received sample shows a different O 1s spectral shape. In order to estimate the main contributions to the native oxide composition, this spectrum was compared with that found in previous works for TiO_2, TiO, Ti_2O_3, ZrO_2 and Nb_2O_5.[26,27] The spectrum of the as-received Ti13Nb13Zr alloy presents features that are similar to those of Ti_2O_3, although a mixture of different titanium oxides is also possible. Additionally, a small contribution of Zr and Nb oxides cannot be excluded. In a previous work performed on the passive layer of these Ti alloys by XPS, the presence of Zr oxides was observed but no Nb emission was detected.[9] However, owing to the different probing depth of XAS and XPS, a comparison of the results obtained by both techniques should be done carefully.

Both O 1s and Ti 2p XAS spectra of the Ti–13Nb–13Zr heat-treated samples indicate that the oxide layer formed on this alloy is rutile (TiO_2). Thus, the previous Ti/O calculation could help to confirm the presence of metallic titanium in the Ti 2p XAS spectrum of the as-received sample. The relative Ti 2p/O 1s absorption intensity obtained for the 24-h heat-treated alloy would correspond to TiO_2, as deduced from the XAS spectral shapes. As mentioned above, the calculated Ti/O ratio gives a slightly higher value for the as-received sample. This result would indicate that for this sample there is Ti 2p emission of non-oxidized Ti, i.e. of metallic titanium.

For the Ti–15Zr–4Nb alloy, the Ti 2p and O 1s XAS spectra of the as-received and heat-treated samples are shown in Figs 4 and 5, respectively. In these figures, the same behaviour as in the Ti–13Nb–13Zr alloy is observed. All heat-treated Ti–15Zr–4Nb samples exhibit the typical spectrum of rutile (TiO_2). The as-received alloy spectrum is quite similar to that of the Ti–13Nb–13Zr sample, showing a small metallic contribution and the native oxide shape, suggesting also a Ti_2O_3 layer and not excluding the presence of other Ti, Zr or Nb oxides. Again, the Ti/O ratio for this sample is slightly higher than that corresponding to TiO_2. This confirms once more the contribution of metallic Ti from the region below the passive layer.

The XAS spectra of the TiNbZr alloys suggest that in both cases the passive layer formed spontaneously by air contact is composed mainly of Ti_2O_3. The Nb and Zr incorporation into the passive film cannot be excluded, although its contribution would be very low. For all heat-treated samples, even for the shortest treatment time, i.e. 90 min, the spectra reveal an oxide film formed by TiO_2 in the form of rutile.

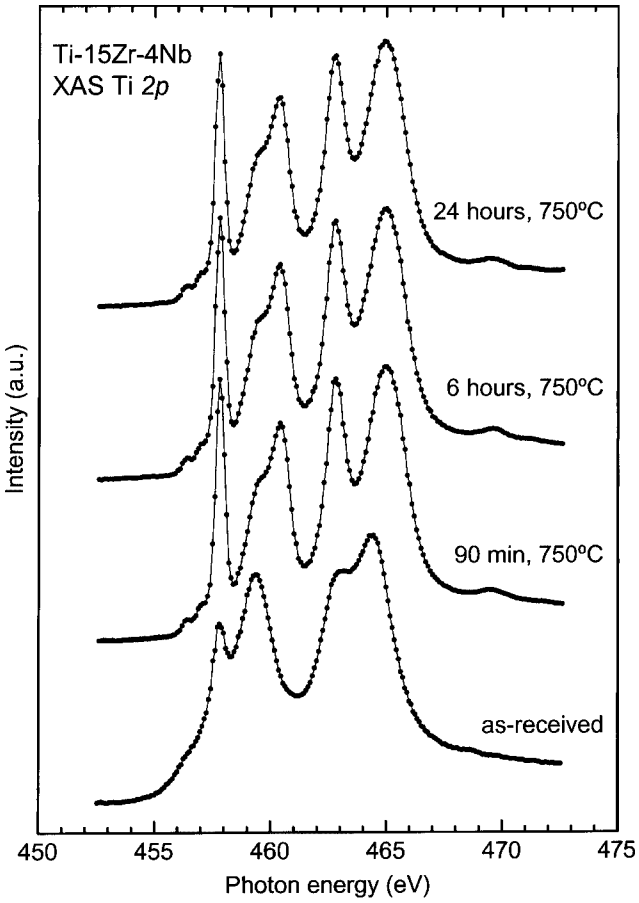

Figure 4. Titanium 2p soft x-ray absorption spectra of the as-received and heat-treated Ti–15Zr–4Nb alloy.

The TiNbAl alloy

The Ti 2p XAS spectra of the as-received and heat-treated Ti–7Nb–6Al alloy are shown in Fig. 6. All heat-treated alloy spectra are very similar, but their shape is different to that of the spectra of heat-treated TiNbZr alloys. For instance, the shoulder of the e_g peak is not observed. A comparison of these spectra with those of previous works leads to the conclusion that they correspond to Al_2TiO_5.[29] Thus, the oxidation process of Ti–7Nb–6Al promotes the formation of Al_2TiO_5, contrary to TiNbZr alloys where TiO_2 was formed. The as-received Ti–7Nb–6Al alloy spectrum is, however, similar to that of TiNbZr alloys.

Figure 7 represents the O 1s XAS spectra of the as-received and heat-treated Ti–7Nb–6Al alloy. In contrast with the TiNbZr alloys spectra, for the heat-treated samples a broad feature at ~540 eV is observed. As mentioned above, this energy region can be assigned to O 2p states hybridized with Ti 4s and 4p states. On the other hand, Al 3s and 3p states hybridized with O 2p states also should be present in this case. By comparing the spectral shape of the heat-treated samples with that of previous works, it can be concluded that this broad structure corresponds to Al_2O_3.[29] The intensity of this feature increases on increasing the treatment time. Additionally, two peaks appear at ~531 eV and ~533.5 eV, which correspond to the e_g and t_{2g} orbitals, respectively, of the Ti 3d states hybridized with O 2p states. Taking into account the Ti 2p spectra, these peaks would correspond

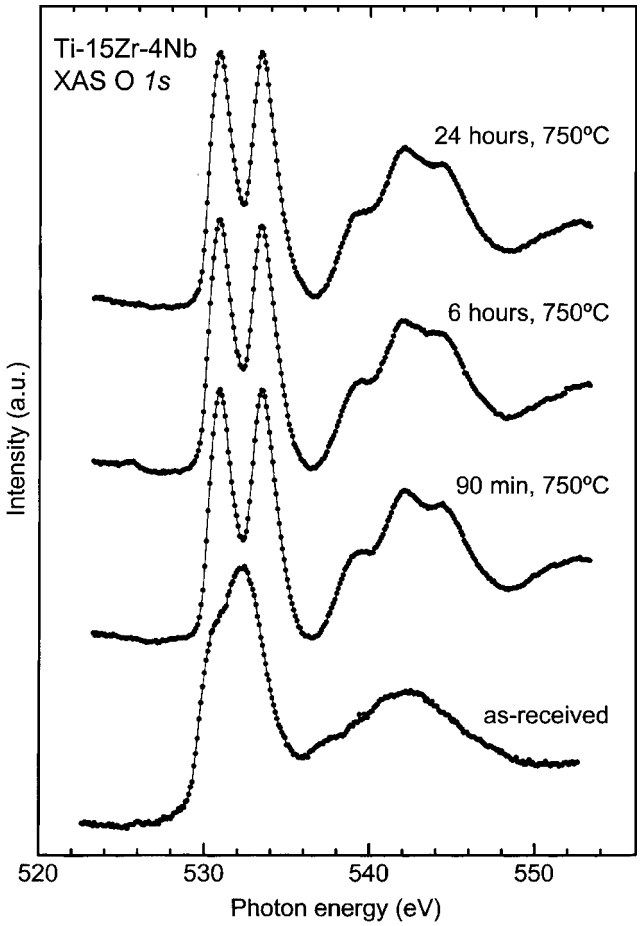

Figure 5. Oxygen 1s soft x-ray absorption spectra of the as-received and heat-treated Ti–15Zr–4Nb alloy.

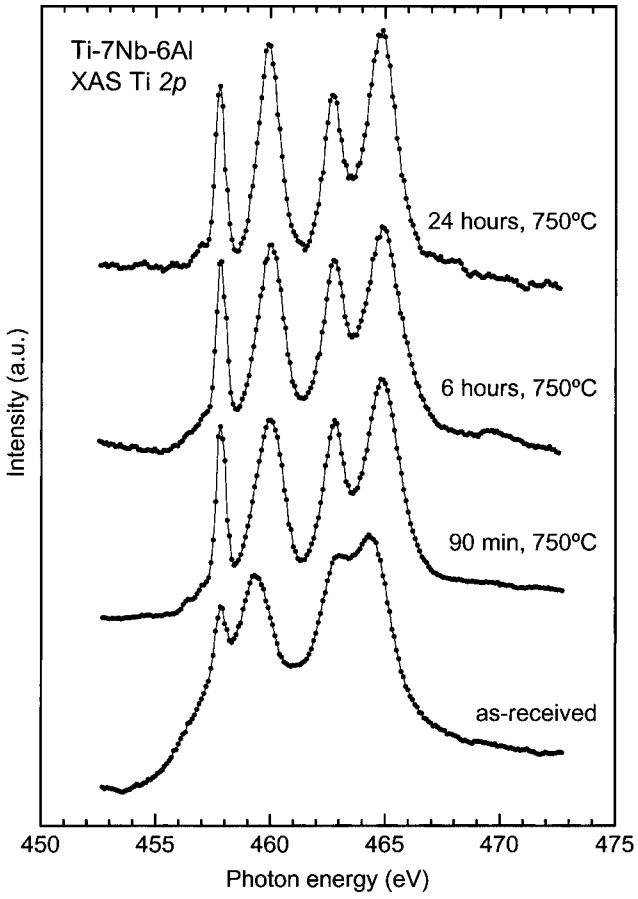

Figure 6. Titanium 2p soft x-ray absorption spectra of the as-received and heat-treated Ti–7Nb–6Al alloy.

to the Al_2TiO_5 emission, which decreases on increasing the treatment time. These results suggest that the early state of oxidation promotes the formation of an Al_2TiO_5 layer on the material. As the exposure time increases, an Al_2O_3 layer grows on the previous oxide, suggesting a favoured Al diffusion by the thermal process. Afterwards, by increasing the heat treatment time, this Al_2O_3 layer becomes thicker, as deduced from the continuous enhancement of the Al 4s–4p feature corresponding to Al_2O_3. In previous works on other metallic materials also having low Al content, preferential Al_2O_3 formation by heat treatment was also observed.[21] As can be seen in Fig. 7, the native oxide spectrum of Ti–7Nb–6AI is similar to that of TiNbZr alloys. Additionally, an emerging feature relative to O 2p hybridized with Al 4s and 4p states can be observed. This spectral shape suggests a passive layer formed mainly by Ti_2O_3 with a small Al_2TiO_5 contribution. Again, the presence of other Ti oxides cannot be excluded.

As for the TiNbZr alloys, the Ti/O ratio calculated from the survey spectra can give additional information about the Ti–7Nb–6Al oxidation process. In contrast to TiNbZr alloys, where the Ti/O ratio was slightly higher for the as-received sample than for the heat-treated samples, the Ti–7Nb–6Al spectra exhibit a strong Ti/O decrease as oxidation proceeds. Also, the Ti/O value further decreases on increasing the oxidation time. This is an indication of the continuous oxidation of elements other than Ti. In the early stage of oxidation, the Ti/O decrease can be associated with the formation of the Al_2TiO_5 layer on the material. As the treatment time increases, an Al_2O_3 layer grows on the Al_2TiO_5 film, leading to a new strong decrease of the Ti/O ratio. Finally, as the Al_2O_3 layer becomes thicker the Ti/O ratio decreases again. Thus, this behaviour suggested from the Ti/O estimation is a confirmation of the oxidation mechanism concluded from the Ti 2p and O 1s spectra.

DISCUSSION

For the three titanium alloys, the XAS experiments of the as-received samples show a passive layer formed mainly by Ti_2O_3. The high atomic per cent of Ti in the Ti alloy composition promotes the preferential formation of Ti_2O_3 on the alloys. In the Ti–7Nb–6Al alloy, the presence of a small amount of Al_2TiO_5 was also observed. Furthermore, a small contribution of other oxides in these passive layers cannot be excluded.

For the oxide layers formed on the alloys by heat treatment, the XAS experiments suggest a different oxidation behaviour for the TiNbZr alloys and for Ti–7Nb–6Al. In the case of the TiNbZr alloys the oxide layer formed on the material is mainly rutile (TiO_2). However, for Ti–7Nb–6Al the early stage of the oxidation process leads to the formation of an Al_2TiO_5 layer. Then, on increasing the treatment time, Al_2O_3 grows on this initial film.

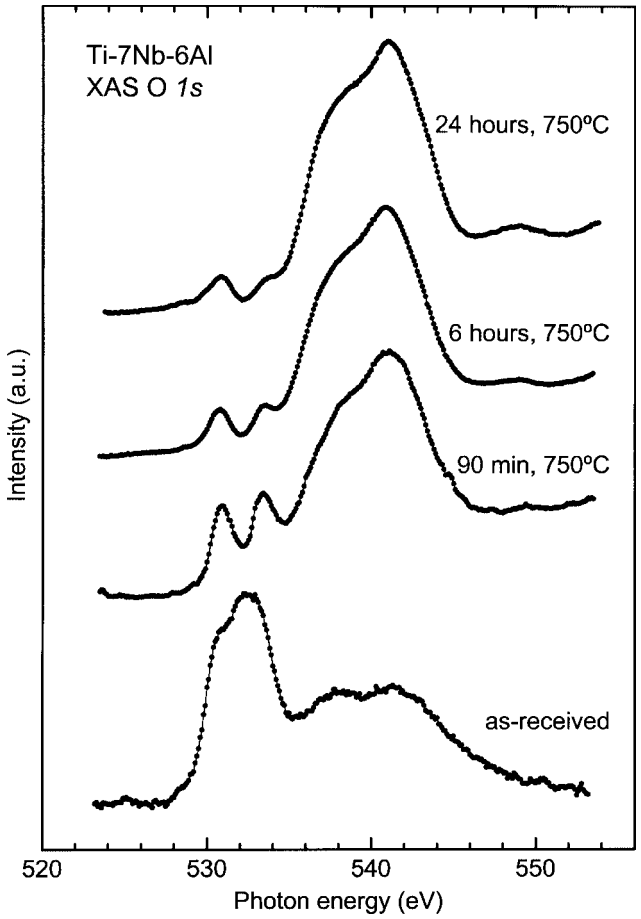

Figure 7. Oxygen 1s soft x-ray absorption spectra of the as-received and heat-treated Ti–7Nb–6Al alloy.

Ellingham's diagram—standard free energies of formation of oxides as a function of temperature—shows that Al and Zr oxidation is thermodynamically favoured compared with Ti oxidation.[30] However, the TiNbZr alloys exhibit by a preferential oxidation of Ti heat treatment, as observed by XAS. This unexpected behaviour reveals that other important parameters should be taken into account to determine the oxidation behaviour: the atomic composition of the substrate and the alloying element diffusion inside the oxide layer. In the TiNbZr alloys, the high content of Ti in the substrate compared with that of Zr leads to the initial formation of rutile (TiO_2) in the oxidation process. Then, as the XAS results reveal, on increasing the treatment time Ti diffusion inside the TiO_2 layer is favoured with respect to Zr diffusion from the substrate to the surface. This effect leads to continuous growth of the TiO_2 layer. Thus, although the oxidation of Zr is thermodynamically favoured versus Ti oxidation, the composition of the alloys and the element diffusion inside the oxide layers determine the oxidation behaviour.

For Ti–7Nb–6Al, the oxidation process thermodynamically favours Al oxidation versus Ti oxidation. However, the high content of Ti compared with Al in the alloy composition gives rise in the initial oxidation process to the formation of an Al_2TiO_5 layer. As the oxidation time increases, the XAS spectra exhibit the presence of an Al_2O_3 signal that increases continuously. This result indicates that the diffusion of Al inside the Al_2TiO_5 layer is larger than that of Ti. Furthermore, as mentioned above, for Ti–7Nb–6Al the oxidation treatment thermodynamically promotes the Al oxidation, leading to the observed formation of the Al_2O_3 layer.

CONCLUSIONS

In order to perform a chemical analysis of the passive and oxide layers formed on Ti–13Nb–13Zr, Ti–15Zr–4Nb and Ti–7Nb–6Al alloys, the XAS spectra were measured. The passive films studied were formed spontaneously on the alloys through air contact at room temperature. The oxide layers were obtained by thermal treatment at 750 °C for three different exposure times. To carry out this investigation, O 1s and Ti 2p XAS spectra were measured. The XAS spectra of as-received samples were similar for the three alloys, suggesting the presence of the native oxide composed mainly of Ti_2O_3. Furthermore, the presence of a small Al_2TiO_5 contribution was observed in the case of the Ti–7Nb–6Al alloy.

The spectra of the heat-treated samples are similar for TiNbZr alloys but Ti–7Nb–6Al has a different behaviour. The oxide film formed on the TiNbZr alloys is clearly TiO_2 in the form of rutile. The high Ti content in the alloy composition as well as the favoured Ti diffusion inside the oxide layers are the main factors responsible for the TiO_2 film formation.

In the case of the Ti–7Nb–6Al alloys, the presence of Al in the chemical composition leads to a different oxidation tendency. In this sample, as oxidation proceeds, the small Al_2TiO_5 contribution of the native oxide layer becomes larger. On increasing the treatment time an Al_2O_3 film grows on the initial oxide layer, becoming continuously thicker. Thus, the formation of Al_2O_3 on this alloy is favoured by the thermal treatment.

The results of this work show the importance of both the alloying elements and the element diffusion in the oxidation behaviour of Ti alloys. Furthermore, this investigation confirms that XAS is an appropriate technique to provide information on the chemical and electronic properties of passive and oxide layers. The different oxidation mechanisms between TiNbZr alloys and Ti–7Nb–6Al have been determined clearly by this spectroscopic technique.

Acknowledgements

This work has been supported financially by Project 07N-0050-1999 of the Spanish 'Programa de Tecnología de los Materiales de la Comunidad Autónoma de Madrid', the MCYT of Spain (BFM2000-0023) and the EU-HPP programme (contract number HPRI-CT-1999-00028). Technical assistance by the BESSY staff is gratefully acknowledged. One of the authors (A. G.) thanks the Spanish Ministerio de Ciencia y Tecnología for financial support through the ''Ramón y Cajal'' programme.

REFERENCES

1. Sibum H, Güther V, Roidl O. In *Alloys*, F. Habashi (ed.). Wiley-VCH: Weinheim, 1998; 213–219.
2. Boyer R, Welsch G, Collings EE. *Materials Properties Handbook: Titanium Alloys*. ASM International: Materials Park, OH, 1994.
3. Froes FH, Yau TL, Weidinger HG. In *Structure and Properties on Nonferrous Alloys*, vol. 8, Cahn RW, Haasen P, Kramer EJ (eds). Serie Materials Science and Technology. VCH: Weinheim, 1996; 403–434.

4. Park JB. In *The Biomedical Engineering Handbook*, Bronzino JD (ed.). CRC Press: Boca Raton, FL, 1995; 540–543.
5. Breme HJ, Biehl V, Helsen JA. In *Metals as Biomaterials*, Helsen JA, Breme HJ (eds). John Wiley: Chichester, 1998; 40–71.
6. Kohn DH, Ducheyne P. In *Medical and Dental Materials*, vol. 14, Williams DF (ed.). Serie Materials Science and Technology. VCH: Weinheim, 1992; 31–45.
7. Okazaki Y, Rao S, Ito Y, Tateishi T. *Biomaterials* 1998; **19**: 1197.
8. Ong JL, Lucas LC. *Biomaterials* 1998; **19**: 455.
9. López MF, Gutiérrez A, Jiménez JA. *Surf. Sci.* 2001; **482**: 300.
10. de Groot FMF. *J. Electron Spectrosc.* 1994; **67**: 529.
11. Soriano L, Abbate M, Fuggle JC, Prieto P, Jiménez C, Sanz JM, Galán L, Hofmann S. *J. Vac. Sci. Technol. A* 1993; **11**: 47.
12. Gutiérrez A, López MF, Pérez Trujillo FJ, Hierro MP, Pedraza F. *Surf. Interface Anal.* 2000; **30**: 130.
13. López MF, Gutiérrez A, Pérez Trujillo FJ, Hierro MP, Pedraza F. *J. Electron Spectrosc.* 2001; **114**: 825.
14. López MF, Gutiérrez A, Torres CL, Bastidas JM. *J. Mater. Res.* 1999; **15**: 763.
15. Bastidas JM, López MF, Gutiérrez A, Torres CL. *Corros. Sci.* 1998; **40**: 431.
16. Gutiérrez A, López MF, García I, Vázquez A. *J. Vac. Sci. Technol. A* 1997; **15**: 294.
17. Abbate M, Goedkoop JB, De Groot FMF, Grioni M, Fuggle JC, Hofmann S, Petersen H, Sacchi M. *Surf. Interface Anal.* 1992; **18**: 65.
18. Schroeder SLM. *Solid State Commun.* 1996; **98**: 405.
19. Gutiérrez A, Alonso C, López MF, Escudero ML. *Surf. Sci.* 1999; **430**: 206.
20. López MF, Gutiérrez A, García-Alonso MC, Escudero ML. *Solid State Commun.* 1997; **101**: 575.
21. López MF, Gutiérrez A, García-Alonso MC, Escudero ML. *J. Mater. Res.* 1998; **13**: 3411.
22. de Groot FMF, Fuggle JC, Thole BT, Sawatzky GA. *Phys. Rev. B* 1990; **41**: 928.
23. Brydson R, Sauer H, Engel W, Thomas JM, Zeitler E, Kosugi N, Kuroda H. *J. Phys.: Condens. Matter* 1989; **1**: 797.
24. Soriano L, Abbate M, Vogel J, Fuggle JC, Fernández A, González-Elipe AR, Sacchi M, Sanz JM. *Surf. Sci.* 1993; **290**: 427.
25. Soriano L, Abbate M, De Groot FMF, Alders D, Fuggle JC, Hofmann S, Petersen H, Braun W. *Surf. Interface Anal.* 1993; **20**: 21.
26. Lusvardi VS, Barteau MA, Chen JG, Eng J Jr, Frühberger B, Teplyakov A. *Surf. Sci.* 1998; **397**: 237.
27. Soriano L, Abbate M, Fuggle JC, Jiménez MA, Sanz JM, Mythen C, Padmore A. *Solid State Commun.* 1993; **87**: 699.
28. de Groot FMF, Faber J, Michiels JJM, Czyzyk MT, Abbate M, Fuggle JC. *Phys. Rev. B* 1993; **48**: 2074.
29. Soriano L, Abbate M, Fernández A, González-Elipe AR, Sanz JM. *Surf. Interface Anal.* 1997; **25**: 804.
30. Kofstad P. In *High Temperature Corrosion*. Elsevier Applied Science: London, 1988; 4–24.